
JOURNAL OF THE AMERICAN CHEMICAL SOCIETY

Three-Center, Two-Electron Systems. Origin of the Tilting of Their Substituents

Koop Lammertsma*[†] and Tomohiko Ohwada[‡]

Contribution from the Department of Chemistry, University of Alabama at Birmingham, UAB Station, Birmingham, Alabama 35294, and Faculty of Pharmaceutical Sciences, University of Tokyo, 7-3-1 Hongo, Bunkyo-ku, Tokyo 113, Japan

Received January 2, 1996. Revised Manuscript Received June 8, 1996[⊗]

Abstract: The origin of the tilting of the H-substituents of 14 parent three-center, two-electron (3c–2e) systems, $C_2H_3^+$, $C_2H_4^{2+}$, $C_2H_5^+$, $B_2H_3^-$, B_2H_4 , $B_2H_5^-$, $Be_2H_4^{2-}$, $Si_2H_3^+$, $Si_2H_4^{2+}$, $Si_2H_5^+$, $Al_2H_3^-$, Al_2H_4 , $Al_2H_5^-$, and $Mg_2H_4^{2-}$, is analyzed. The mixing of the σ and π orbitals underlies the upward tilt of these hydrogen substituents. Except for the ethyl cation and the ethylene dication, all 3c–2e systems have all their hydrogens on one side of a plane that contains both heavy elements. These elements thus have inverted geometries. It is shown that the geometrical tilt angles between the X–H_i and the X–X bonds of all the 3c–2e electron systems (anions, cations, dianions, dications, and neutrals containing eight different elements of the first and second rows) correlate linearly with the electronegativities of the heavy elements. The electronic structures of these systems are also reported. They highlight the convex curvature of the X–X bonds. All the investigated 3c–2e systems are either minima or transition structures. The minima associated with the transition structures are identified.

Multicenter bonding has intrigued chemists for decades in areas as diverse as carbocations, carboranes, transition metal complexes, and metallic clusters. While variants with multiple centers are also well established, the emphasis in these delocalized systems and the focus of this paper is on three-center, two-electron (3c–2e) bonding. In fact, 3c–2e bonding reached its pinnacle in borane chemistry and again with stable carbocations.¹ As a result, this type of (nonclassical) bonding has become common in the description of chemical structures.

What can be added that is not already known? After all, the ethyl and vinyl cations have been studied in excruciating detail as the prime examples of 3c–2e bonded systems.² These cation studies focused on the stabilization that resulted from a bridging hydrogen, which is the essence that underlies all nonclassical cations.³ What has received much less attention, however, is what happens with the substituents of the 3c–2e bond. Intuitively, one expects that ethylene and acetylene bend upon protonation, resulting in cations with their terminal hydrogens (H_i) directed away from the bridging one (H_b). This, as we will show, is not necessarily the case.

Before we proceed, it is useful to recall pertinent issues in multicenter bonding. Relevant in this context are the three-dimensional aromatic systems of which Hogeveen's CMe_6^{2+}

[†] University of Alabama at Birmingham.

[‡] University of Tokyo.

[⊗] Abstract published in *Advance ACS Abstracts*, July 15, 1996.

(1) Olah, G. A.; Wade, K.; Williams, R. E. *Electron Deficient Boron and Carbon Clusters*; Wiley: New York, 1991. Olah, G. A.; Prakash, G. K. S.; Williams, R. E.; Field, L. D.; Wade, K. *Hypercarbon Chemistry*; Wiley: New York, 1987. For metallic clusters, see: Crabtree, R. H. *The Organic Chemistry of the Transition Metals*; Wiley: New York, 1988.

(2) For example, see: (a) Raghavachari, K.; Whiteside, R. A.; Pople, J. A.; Schleyer, P. v. R. *J. Am. Chem. Soc.* **1981**, *103*, 5649 and references therein. (b) Bohme, D. K.; Mackay, G. I. *J. Am. Chem. Soc.* **1981**, *103*, 2173. (c) Stang, P. J.; Rapport, Z.; Hanack, M.; Subramanian, L. R. *Vinyl Cations*; Academic Press: New York, 1979.

(3) Of the rich literature on nonclassical ions, see, for example: Olah, G. A.; Prakash, G. K. S.; Saunders, M. *Acc. Chem. Res.* **1983**, *16*, 440. Laube, T. *Acc. Chem. Res.* **1995**, *28*, 399.

(4) Hogeveen, H.; Kwant, P. W. *Acc. Chem. Res.* **1975**, *8*, 413. Giordano, C.; Heldeweg, R. F.; Hogeveen, H. *J. Am. Chem. Soc.* **1977**, *99*, 5181.

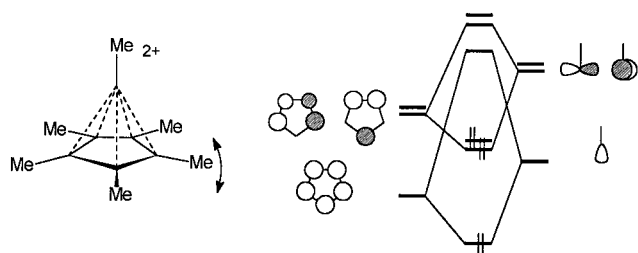


Figure 1. Principle of three-dimensional aromaticity, illustrated for the Hogeveen dication, by the interaction of the Me-C cap with the (CMe)₅ base.

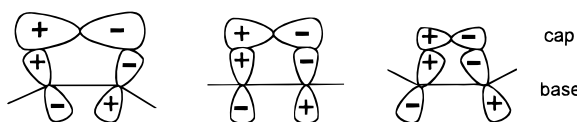


Figure 2. Principle of out-of-plane bending of ring substituents, illustrated for varying sizes of p orbitals of the capping group.

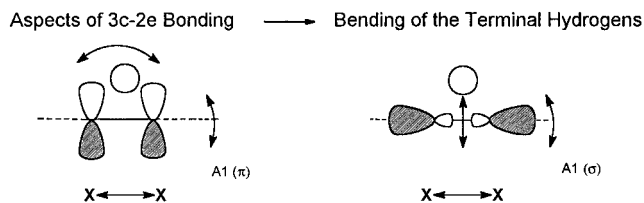


Figure 3. The two contributors influencing the tilting of the olefinic substituents.

dication is the best known example.⁴ Schleyer and Jemmis^{5a} demonstrated for a broad spectrum of mono- and bicapped ring structures the origin of this aromatic stabilization; see Figure 1. They also analyzed the influence of the capping group on the ring substituent. This is illustrated in Figure 2 and is based on the following argument. A capping group with large, diffuse p orbitals requires outward bending of the basal atomic orbitals in the degenerate π MOs and causes a downward tilting of the basal substituents. Conversely, a capping group with small p orbitals requires inward bending of the respective basal MOs and causes upward tilting of the basal substituents.

The question we are asking is whether the analysis for three-dimensional systems is also applicable to the more general 3c–2e systems.^{5b,c} To answer this question we explore the special case of hydrogen-bridged systems. Use of the hydrogen's s orbital alters the emphasis from the cap to the base. The premise of tilting of the substituents remains, though, the same. The characteristics are illustrated in Figure 3, which requires, however, closer scrutiny.

As in Hogeveen's dication there are two types of interactions. First, there is the interaction of the hydrogen s orbital with the π bond of the base. Large, diffuse atomic p orbitals would require outward bending and a downward tilt of the basal substituent. Conversely, small atomic p orbitals would require an inward bend and thereby cause an upward tilt of the basal substituent. Second, there is the interaction of the hydrogen s orbital with the σ bond of the base. This interaction would in all cases tend to tilt the terminal hydrogens downward. Intuitively then the tilt of the substituents depends on the nature

(5) (a) Jemmis, E. D.; Schleyer, P. v. R. *J. Am. Chem. Soc.* **1982**, *104*, 4781 and references cited therein. Jemmis, E. D. *J. Am. Chem. Soc.* **1982**, *104*, 7017. (b) Covalent three-membered-ring structures have been discussed likewise in the context of capped π bonds: Dewar, M. J. S.; Ford, G. P. *J. Am. Chem. Soc.* **1979**, *101*, 783. (c) The effect of the substituent bending angle in carbenium ions and the vinyl cation on 1,2-H shifts has been discussed similarly: Chandrasekhar, J.; Schleyer, P. v. R. *Tetrahedron Lett.* **1979**, 4057. Jemmis, E. D.; Sarma, K. S.; Pavankumar, P. N. V. *THEOCHEM* **1985**, *22*, 305.

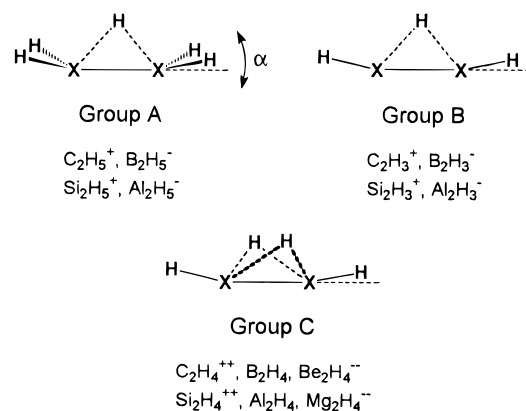


Figure 4. The three groups of this study: A, X₂H₅^{+/-}; B, X₂H₃^{+/-}; and C, X₂H₄^{2+/0/2-}.

of the π bond, *i.e.*, the p orbitals of the elements that form the base. However, these simple arguments are flawed by the fact that they assume constant bond lengths between the heavy elements. This, of course, is far from being the case. How then do we arrive at a qualitative analysis that explains the tilt angle in 3c–2e bonding systems?

To answer this question we examine the three classes of symmetrical 3c–2e systems displayed in Figure 4, *i.e.*, H-bridged double bonds (X₂H₅^{+/-}, group A), H-bridged triple bonds (X₂H₃^{+/-}, group B), and di-H-bridged triple bonds (X₂H₄^{2+/0/2-}, group C) where X = C, B, Be, Si, Al, and Mg. We will demonstrate that the tilting is independent of the charge of the systems. For better insight into the viability of these systems we will also evaluate their relationship with other structures.

Computational Methods

The *ab initio* calculations⁶ were carried out using the GAUSSIAN 92 suite of programs.⁷ Geometries were optimized at the SCF level with the d- and hydrogen p-polarized split-valence 6-31G** basis set and with inclusion of the effects of all electron correlation by using Møller–Plesset perturbation theory at second order using this basis set and the essentially triply split valence basis set 6-311G**. Force constant matrices, vibrational harmonic frequencies, and zero-point energies (ZPE) were calculated analytically for all optimized geometries. Minima are characterized by real frequencies only, while transition structures have one imaginary frequency. Absolute and relative energies are given in Tables 1 and 2, respectively. Throughout the text we use MP2/6-311G** optimized geometries and energies.

The bonding properties of the structures were investigated with Bader's topological one-electron density analysis⁸ using optimized MP2/6-311G** wave functions. The one-electron density distribution $\rho(\mathbf{r})$ was analyzed for each with the aid of the gradient vector field $\nabla\rho(\mathbf{r})$ and the Laplacian $\nabla^2\rho(\mathbf{r})$, which also determines the regions in space wherein electronic charge is concentrated or depleted. Bond critical points are characterized by having a minimum value in $\rho(\mathbf{r})$ along the maximum electron density path connecting two nuclei and are maxima in all other directions. The ellipticity ϵ at such a critical point describes the spatial symmetry of a bond. The properties of the bond critical points are listed in Table 3.

(6) Hehre, W. J.; Radom, L.; Schleyer, P. v. R.; Pople, J. A. *Ab Initio Molecular Orbital Theory*; Wiley: New York, 1986. For orbital interaction schemes, see: Albright, T. A.; Burdett, J. K.; Whangbo, M.-H. *Orbital Interactions in Chemistry*; Wiley: New York, 1985.

(7) Frisch, M. J.; Trucks, G. W.; Head-Gordon, M.; Gill, P. M. W.; Wong, M. W.; Foresman, J. B.; Johnson, B. G.; Schlegel, H. B.; Robb, M. A.; Replogle, E. S.; Gomberts, R.; Andres, J. L.; Raghavachari, K.; Binkley, J. S.; Gonzalez, C.; Martin, R. L.; Fox, D. J.; Defrees, D. J.; Baker, J.; Steward, J. J. P.; Pople, J. A. *GAUSSIAN 92*, revision A; Gaussian, Inc.: Pittsburgh, PA, 1992.

(8) (a) Bader, R. F. W. *Atoms in Molecules—A Quantum Theory*; Oxford: London. (b) Bader, R. F. W. *Acc. Chem. Res.* **1985**, *18*, 9.

Table 1. Absolute Energies (in au) of 3c–2e Systems and Related Structures^a

formula	sym	struct	HF/6-31G**	MP2/6-31G*	MP2/6-311G**	scaled ZPE ^b	MP2/6-311G** + ZPE
C₂H₃⁺	<i>C</i> _{2v}	1-bridge	-77.084 43 (0)	-77.347 33 (0)	-77.401 79 (0, 553.3)	20.708	-77.368 79
Si₂H₃⁺	<i>D</i> _{3h}	3-bridge	-579.223 72 (0)	-579.419 94 (0)	-579.705 91 (0, 521.1)	16.080	-579.680 28
Si₂H₃⁺	<i>C</i> _{2v}	1-bridge	-579.155 44 (2)	-579.349 83 (1)	-579.631 96 (1, -623.0)	13.115	-579.611 06
B₂H₃⁻	<i>C</i> _{2v}	1-bridge	-50.980 88 (0)	-51.189 03 (1)	-51.259 88 (1, -458.4)	16.333	-51.233 85
B₂H₃⁻	<i>C</i> ₂	1-bridge	-50.980 88 (0)	-51.189 25 (0)	-51.260 08 (0, 480.7)	17.189	-51.232 69
B₂H₃⁻	<i>C</i> _{2v}	H ₂ B-BH	-50.985 13 (0)	-51.177 04 (0)	-51.246 37 (0, 239.3)	16.333	-51.220 34
B₂H₃⁻	<i>D</i> _{3h}	3-bridge	-50.901 84 (0)	-51.111 79 (0)	-51.193 29 (0, 955.2)	18.833	-51.163 28
Al₂H₃⁻	<i>D</i> _{3h}	3-bridge	-485.525 21 (0)	-485.687 50 (0)	-485.967 09 (0, 427.7)	13.231	-485.946 01
Al₂H₃⁻	<i>C</i> _{2v}	1-bridge	-485.463 84 (1)	-485.625 80 (1)	-485.909 61 (1, -514.7)	10.984	-485.892 11
C₂H₅⁺	<i>C</i> _{2v}	1-bridge	-78.320 95 (0)	-78.601 18 (0)	-78.655 07 (0, 749.1)	36.921	-78.596 23
Si₂H₅⁺	<i>C</i> _{2v}	1-bridge	-580.423 02 (0)	-580.624 99 (0)	-580.910 83 (0, 340.3)	24.973	-580.871 03
B₂H₅⁻	<i>C</i> _{2v}	1-bridge	-52.220 81 (0)	-52.448 16 (0)	-52.511 77 (0, 541.3)	29.229	-52.465 19
Al₂H₅⁻	<i>C</i> _{2v}	1-bridge	-486.697 86 (0)	-486.873 03 (0)	-487.161 87 (0, 280.0)	20.114	-487.129 82
C₂H₄²⁺	<i>D</i> _{2d}		-77.095 39 (0)	-77.308 12 (0)	-77.356 59 (0, 594.3)	28.162	-77.311 71
C₂H₄²⁺	<i>C</i> _{2v}	2-bridge	-77.025 99 (1)	-77.283 10 (0)	-77.338 79 (0, 350.3)	24.306	-77.300 06
Si₂H₄²⁺	<i>C</i> _{2v}	cyclic	-579.319 72 (0)	-579.498 01 (0)	-579.784 80 (0, 300.2)	19.905	-579.753 08
Si₂H₄²⁺	<i>C</i> _{2v}	2-bridge	-579.256 42 (2)	-579.442 66 (1)	-579.728 01 (1, -320.2)	17.941	-579.699 42
B₂H₄	<i>C</i> _{2v}	2-bridge	-51.607 95 (0)	-51.813 55 (0)	-51.860 58 (0, 461.0)	24.219	-51.821 98
B₂H₄	<i>D</i> _{2d}	H ₂ B-BH ₂	-51.638 59 (0)	-51.815 97 (0)	-51.859 54 (0, 431.7)	23.474	-51.822 13
Al₂H₄	<i>C</i> _{3v}	Al ⁺ AlH ₄ ⁻	-486.095 71 (0)	-486.254 91 (0)	-486.536 61 (0, 400.8)	17.713	-486.508 38
Al₂H₄	<i>C</i> _{2v}	Al ⁺ AlH ₄ ⁻	-486.098 76 (0)	-486.251 69 (0)	-486.533 65 (0, 132.0)	17.482	-486.505 79
Al₂H₄	<i>C</i> _{2v}	2-bridge	-486.055 30 (1)	-486.214 36 (1)	-486.495 85 (1, -159.8)	16.562	-486.469 46
Be₂H₄²⁻	<i>C</i> _{2v}	2-bridge	-31.302 44 (0)	-31.458 02 (0)	-31.554 13 (0, 307.2)	17.170	-31.526 77
Mg₂H₄²⁻	<i>C</i> _{2v}	cyclic	-401.341 76 (0)	-401.467 63 (0)	-401.760 18 (0, 172.4)	12.206	-401.740 73
Mg₂H₄²⁻	<i>C</i> _{2v}	2-bridge	-401.303 03 (1)	-401.435 91 (0)	-401.730 17 (1, -19.2)	11.803	-401.711 36
C₂H₂	<i>D</i> _{∞h}	acetylene	-76.821 84 (0)	-77.091 46 (0)	-77.151 66 (0, 486.7)	15.559	-77.126 87
Si₂H₂	<i>C</i> _{2v}	2-bridge	-578.891 34 (0)	-579.087 55 (0)	-579.369 26 (0, 533.1)	10.087	-579.353 19
C₂H₄	<i>D</i> _{2h}	ethylene	-78.038 84 (0)	-78.327 23 (0)	-78.385 88 (0, 831.7)	30.619	-78.337 09
Si₂H₄	<i>C</i> _{2h}	silylene	-580.082 79 (0)	-580.292 55 (0)	-580.576 35 (0, 354.1)	19.362	-580.545 49
B₂H₆	<i>D</i> _{2h}	diborane	-52.819 86 (0)	-53.048 90 (0)	-53.094 66 (0, 361.0)	38.358	-53.033 53
Al₂H₆	<i>D</i> _{2h}	dialane	-487.281 30 (0)	-487.455 53 (0)	-487.743 13 (0, 225.8)	27.302	-487.699 62

^a Formula entries in boldface are 3c–2e systems. The entries in parentheses indicate the number of imaginary frequencies. For MP2/6-311G** also the smallest (imaginary) frequency is given. ^b The 0.95 scaled zero-point vibrational energies (in kcal/mol) at MP2/6-311G**.

Table 2. Relative Energies (in kcal/mol) of 3c–2e Systems^a

struct	sym	HF/ 6-31G**	MP2/ 6-31G**	MP2/ 6-311G**	MP2/ 6-311G** + ZPE
B₂H₃⁻	<i>C</i> ₂ (0)	2.67	0.00	0.00	0.00
B₂H₃⁻	<i>C</i> _{2v} (1)	2.67	0.14	0.13	-0.73
B₂H₃⁻	<i>C</i> _{2v} (0)	0.00	7.66	8.60	7.75
B₂H₃⁻	<i>D</i> _{3h} (0)	52.27	48.61	41.91	43.56
Al₂H₃⁻	<i>D</i> _{3h} (0)	0.00	0.00	0.00	0.00
Al₂H₃⁻	<i>C</i> _{2v} (1)	38.51	38.72	36.07	33.82
Si₂H₃⁺	<i>D</i> _{3h} (0)	0.00	0.00	0.00	0.00
Si₂H₃⁺	<i>C</i> _{2v} (1)	42.85	43.99	46.40	43.44
B₂H₄	<i>C</i> _{2v} (0)	19.23	-1.52	-0.65	-1.14
B₂H₄	<i>D</i> _{2d} (0)	0.00	0.00	0.00	0.00
C₂H₄²⁺	<i>D</i> _{2d} (0)	0.00	0.00	0.00	0.00
C₂H₄²⁺	<i>C</i> _{2v} (0)	43.55	15.7	11.12	7.31
Si₂H₄²⁺	<i>C</i> _{2v} (0)	0.00	0.00	0.00	0.00
Si₂H₄²⁺	<i>C</i> _{2v} (1)	39.72	34.73	35.64	33.67
Al₂H₄	<i>C</i> _{3v} (0)	1.91	0.00	0.00	0.00
Al₂H₄	<i>C</i> _{2v} (0)	0.00	2.02	1.86	1.63
Al₂H₄	<i>C</i> _{2v} (1)	27.27	25.45	25.58	24.42
Mg₂H₄²⁻	<i>C</i> _{2v} (0)	0.00	0.00	0.00	0.00
Mg₂H₄²⁻	<i>C</i> _{2v} (1)	24.30	19.90	18.83	18.43

^a See footnote a of Table 1.

Results and Discussion

The discussion consists of analyses of the structures, their electron densities, and their energies. In the first part, the posed question of the tilting of the substituents of the 3c–2e systems is answered. In the second part, a more detailed analysis of the bonding properties is presented that relates the 3c–2e systems to other so-called electron-deficient systems. Finally, the relevance of several 3c–2e systems is discussed.

I. Geometries. The geometrical parameters of the 3c–2e structures, optimized at MP2/6-311G**, are summarized in Figure 5. The geometrical tilt angles of the terminal hydrogens of the structures of the three groups are given in Figure 6. The tilt angle is defined as the angle between the H_iXH_i plane or H_i–X bond with the X–X bond. These angles are quite substantial, with a spread of ca. 15° for the mono-H-bridged structures of groups A and B and an even larger spread of 22° for the di-H-bridged structures of group C. Still more surprising is that all structures have their terminal hydrogens (H_i) tilted upward, except for the cations C₂H₄²⁺ and C₂H₅⁺, which have these hydrogens marginally tilted downward. Thus, except for these two cases, all hydrogens are located on one side of the plane orthogonal to the X₂H_b plane and containing the heavy elements (see Figure 7). Such a bonding arrangement seems perplexing. It suggests that the geometries of the “sp²/sp²-hybridized” X atoms are inverted! While such features have been discussed for “inverted sp³-carbons” by Wiberg⁹ and for “inverted sp²-carbons” by Lammertsma,¹⁰ they are not expected to play a role in the unconstrained systems of the present study.

Let us return to the arguments outlined in the introduction and focus on the σ (A₁) and π (A₁) orbitals shown in Figure 3. If the tilting of the substituents is controlled by these orbitals, such an effect should be reflected in their energies. Intuitively, it is expected that the tilting is dominated by the π orbital, which is the HOMO. To verify this we changed the tilt angle of the terminal hydrogens of C₂H₅⁺, Si₂H₅⁺, and Al₂H₅⁻ from -10° to up to 20° while optimizing all other parameters. The strongest influence for each of the three systems is on the

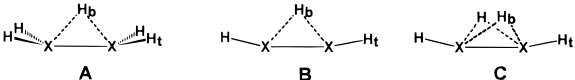
(9) Wiberg, K. B.; Walker, F. H. *J. Am. Chem. Soc.* **1982**, *104*, 5239. Wiberg, K. B. *J. Am. Chem. Soc.* **1983**, *105*, 1227. Wiberg, K. B.; Bader, R. F. W.; Lau, C. D. H. *J. Am. Chem. Soc.* **1987**, *109*, 985, 1001.

(10) Lammertsma, K. *J. Am. Chem. Soc.* **1986**, *108*, 5127.

Table 3. MP2/6-311G** Critical Point Data for $X_2H_3^{+/-}$, $X_2H_5^{+/-}$, and $X_2H_4^{2+/0/2-}$ ^{a,b}

struct	type	ϵ	ρ	$\nabla^2\rho$	struct	type	ϵ	ρ	$\nabla^2\rho$
$C_2H_3^+$	C-C	0.316	2.661	-2.942	$B_2H_3^-$	B-M	0.189	1.213	-7.508
	C ₂ -H _b	0.652	1.395	-7.922		M	0.138	1.217	-9.397
	C-H _t	0.017	1.939	-29.221		B ₂ -H _b	0.588	0.983	-2.246
$Si_2H_3^+$	Si-M	1.179	0.723	1.224	$Al_2H_3^-$	Al-M	0.472	0.367	0.372
	M	1.040	0.744	-4.170		M	0.483	0.375	-1.519
	Si ₂ -H _b	0.156	0.618	-0.072		Al ₂ -H _b	0.355	0.345	-0.219
	Si-H _t	0.048	0.880	5.624		Al-H _t	0.035	0.523	6.970
$C_2H_5^+$	C-C	0.236	2.162	-23.968	$B_2H_5^-$	B-B	0.562	1.086	-8.884
	C ₂ -H _b	1.578	1.300	-6.975		B ₂ -H _b	2.026	0.931	-3.237
	C-H _t	0.019	1.992	-27.663		B-H _t	0.223	1.047	-0.184
$Si_2H_5^+$	Si-M	0.457	0.703	-2.203	$Al_2H_5^-$	Al-M	0.844	0.365	-0.233
	M	0.414	0.715	-4.981		M	0.763	0.376	-1.956
	Si ₂ -H _b	4.023	0.596	-0.880		Al ₂ -H _b	1.237	0.354	-0.889
	Si-H _t	0.035	0.878	6.789		Al-H _t	0.027	0.493	6.628
$C_2H_4^{2+}$	C-C	0.028	2.578	-29.779	B_2H_4	B-B	0.059	1.215	-8.217
	C ₂ -H _b	0.677	1.253	-9.168		M	0.098	1.218	-9.290
	C-H _t	0.004	1.752	-29.273		B ₂ -H _b	0.974	1.025	-3.105
	Si-M	0.057	0.708	-1.538		Al-Al	0.015	0.368	0.060
$Si_2H_4^{2+}$	M	0.188	0.719	-4.370	Al_2H_4	M	0.258	0.377	-1.695
	Si ₂ -H _b	2.142	0.611	-0.512		Al ₂ -H _b	0.323	0.349	-0.407
	Si-H _t	0.010	0.903	3.252		Al-H _t	0.012	0.569	7.481
	Be-H _b	0.294	0.390	5.579		Mg-H _b	0.064	0.198	3.090
BeH_4^{2-}	Be-H _t	0.049	0.467	4.890	$Mg_2H_4^{2-}$	Mg-H _t	0.017	0.271	4.138
	H _b -H _b	0.308	0.359	0.485		H _b -H _b	0.181	0.141	0.469

^a Bond critical point data are given for the identified bond path, except for M, which is a maximum on the X-X bond path. For a description of ϵ see the text in the methods section. ρ values are in $e/\text{\AA}^3$. $\nabla^2\rho$ values are in $e/\text{\AA}^5$. ^b No ring critical points are given for the dianions nor for $Al_2H_3^-$, which has additional Al-H_b bond paths with $\epsilon = 0.707$, $\rho = 0.347 e/\text{\AA}^3$, and $\nabla^2\rho = 4.396 e/\text{\AA}^5$.

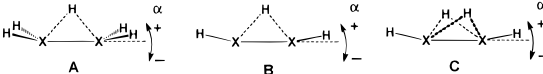


The Interatomic Distances

	C-C	B-B	Si-Si	Al-Al	Be-Be	Mg-Mg
A $X_2H_3^{+/-}$	1.384	1.624	2.192	2.439		
B $X_2H_5^{+/-}$	1.234	1.466	1.997	2.237		
C $X_2H_4^{2+/0/2-}$	1.266	1.470	2.055	2.231	1.899	2.638

	C-H _t	B-H _t	Si-H _t	Al-H _t	Be-H _t	Mg-H _t
A $X_2H_3^{+/-}$	1.087	1.217	1.454	1.609		
B $X_2H_5^{+/-}$	1.080	1.190		1.582		
C $X_2H_4^{2+/0/2-}$		1.172	1.476	1.558	1.413	1.807

	C-H _b	B-H _b	Si-H _b	Al-H _b	Be-H _b	Mg-H _b
A $X_2H_3^{+/-}$	1.311	1.375	1.692	1.805		
B $X_2H_5^{+/-}$	1.282	1.344	1.658	1.782		
C $X_2H_4^{2+/0/2-}$	1.349	1.345	1.677	1.770	1.493	1.954

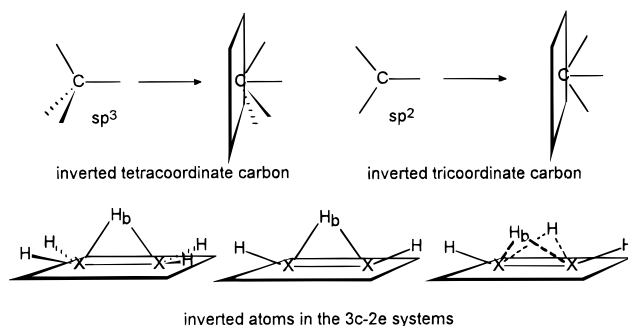
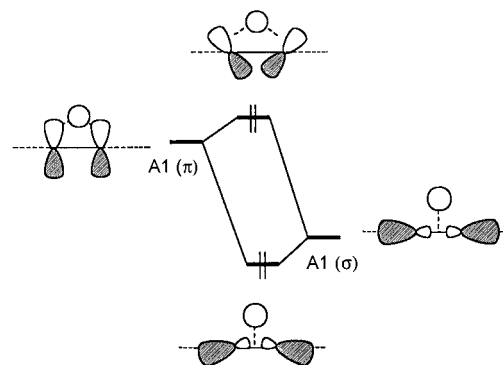
Figure 5. MP2(full)/6-311G** optimized bond lengths of the 3c-2e systems.


The Tilt Angle of the Substituents

Electroneg.	A	α	B	α	C	α	
C	2.55	$C_2H_3^+$	-0.5	$C_2H_3^+$	0.3	$C_2H_4^{2+}$	-2.1
B	2.04	$B_2H_3^-$	4.5	$B_2H_3^-$	7.2	$Be_2H_4^{2-}$	6.3
Si	1.90	$Si_2H_3^+$	11.6	$Si_2H_3^+$	12.7	$Si_2H_4^{2+}$	15.2
Al	1.61	$Al_2H_3^-$	13.7	$Al_2H_3^-$	15.2	Al_2H_4	17.2
Be	1.57					$Be_2H_4^{2-}$	13.8
Mg	1.31					$Mg_2H_4^{2-}$	19.8

Figure 6. MP2(full)/6-311G** optimized geometrical tilt angles of the 3c-2e systems.

energies of both the π (HOMO) and σ (HOMO - 2 or 3) orbitals, but in opposite directions. The upward tilting (*i.e.*, H_t moving closer to H_b) is favored by the π orbital and disfavored

**Figure 7.** Inverted geometries of carbon and other elements in the 3c-2e systems.**Figure 8.** Interaction diagram for the π and σ (A_1) orbitals of the 3c-2e systems.

by the σ orbital. What complicates matters further is the mixing of these two A_1 -symmetry orbitals, the extent of which depends on the degree of tilting. Figure 8 shows a mixing diagram. Figure 9 shows the respective orbitals for $C_2H_5^+$ and $Si_2H_5^+$ and illustrates the occurrence of mixing in the silicium ion. The mixing of orbitals of like symmetry is more prominent on closer spacing of their energy levels. This of course is the case for the heavier elements down the column of the periodic table. The upward tilting of the terminal hydrogens is particularly

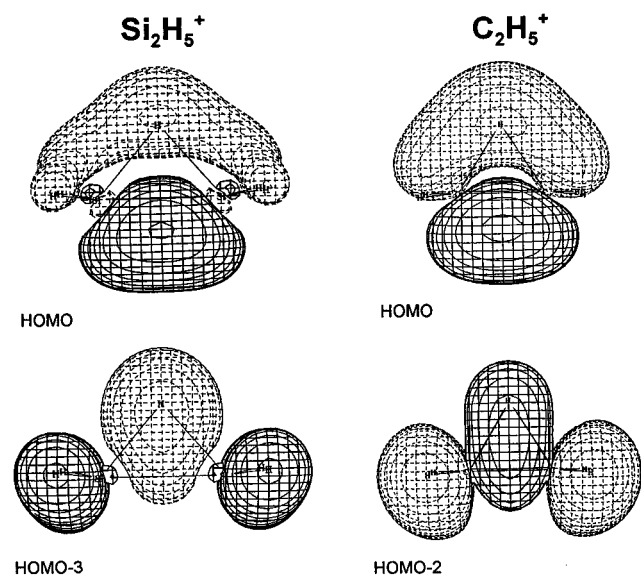


Figure 9. The π and ρ (A_1) orbitals for Si_2H_5^+ (on the left-hand side) and C_2H_5^+ .

facilitated by strong mixing of the π and σ (CH_2) orbitals because this maximizes their bonding interactions. The comparison of Si_2H_5^+ with C_2H_5^+ is illustrative.

The distance between the elements X further influences the above discussed interactions. Expectantly, the effect is largest on changing the elements, and the dramatic variations in X–X bond distances, summarized in Figure 5, reflect this. For the same element, however, the variation in the X–X distances between the different groups A, B, and C is modest and reflects the degree of multiple bonding. It is well recognized that the length of a covalent bond is related to the electronegativity of its elements. The 3c–2e species of this study should be no exception, and indeed they follow the expected trend. Thus, the B–B bond lengths are longer than the C–C bonds and the Be–Be bond is longer still. The same trend holds for the X–X bonds of the second-row elements.

As the covalent X–X bond lengths are related to the electronegativities of the elements and as the degree of π overlap relates to the polarizability of the elements, should then the bonding in the hydrogen-bridged 3c–2e systems not show a similar relationship? This can indeed be substantiated. *All tilt angles correlate exceptionally well with Allred and Rochow's¹¹ elemental electronegativities!* This is shown in Figure 10 ($r = 0.971$). Likewise, the suggested correlation of the tilting angles with the X–X bond lengths is found to be remarkably good, and this is shown in Figure 11 (first row, $r = 0.943$; second row, $r = 0.899$). These correlations are indeed astonishing considering that the data set is composed of three different types of 3c–2e species that include neutral species and singly and doubly charged cations and anions of the first and second rows of the periodic table!

II. Electron Densities. Now that we have demonstrated that the tilt angles of terminal hydrogens of 3c–2e species correlate with such a fundamental concept as elemental electronegativities, the validity of this correlation requires further inspection. This relationship between the tilt angle and electronegativity could, for example, be a fortuitous one. Are we dealing with fact or fiction? In attempting to address this question it must be realized that the tilt angle is a geometrical parameter of the 3c–2e species. The tilt is the angle between the X– H_i bond or

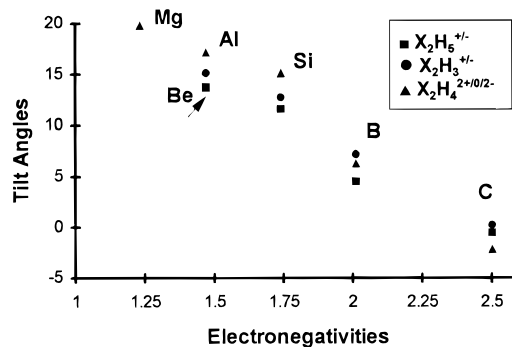


Figure 10. Correlation between H_i tilt angles and Allred and Rochow's elemental electronegativities. The element X is identified and located in the graph next to the entries of the three 3c–2e systems $\text{X}_2\text{H}_5^{+/-}$ (■), $\text{X}_2\text{H}_3^{+/-}$ (●), and $\text{X}_2\text{H}_4^{2+/0/2-}$ (▲), except for Be and Mg, for which only the dianions are shown.

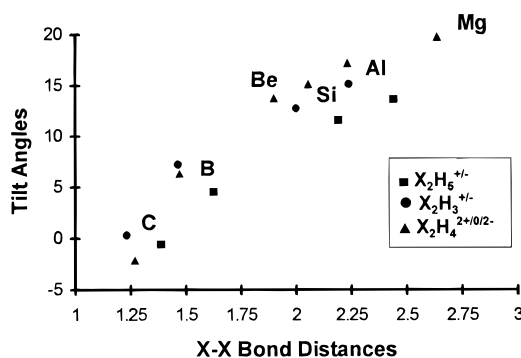


Figure 11. Correlation between X–X bond lengths and H_i tilt angles. Each element X is identified and located in the graph next to the entries of the three 3c–2e systems $\text{X}_2\text{H}_5^{+/-}$ (■), $\text{X}_2\text{H}_3^{+/-}$ (●), and $\text{X}_2\text{H}_4^{2+/0/2-}$ (▲), except for Be and Mg, for which only the dianions are shown.

X(H_i)₂ plane and the X–X bond. This definition leads, as already noted, to the unexpected inverted geometries of di- and trivalent atoms. While such geometries may have merit in small clusters, they are an unfamiliar feature in unstrained hydrocarbons. What then determines this behavior? The answer must lie in the nature of the X– H_i and/or X–X bonds. It is well established that bonds can be curved, like in the strained C–C bonds in cyclopropane, but can this also be the case for the unstrained X–X bonds in the 3c–2e species?

This matter can be elucidated by determining for all the species of groups A, B, and C their bond paths with Bader's topological one-electron density analysis. These bond paths are the paths of maximum electron density connecting two nuclei. Representative molecular graphs are shown in Figure 12. These graphs reveal several features pertinent to the 3c–2e bonding.

The X–X bond in each of the molecular graphs is highly curved in such a manner that in all the 3c–2e systems the bonds departing from X are either virtually collinear, as in $\text{X}_2\text{H}_3^{+/-}$ and $\text{X}_2\text{H}_4^{2+/0/2-}$, or coplanar, as in $\text{X}_2\text{H}_5^{+/-}$. Consequently, *neither of these molecular graphs shows tilt angles for the terminal hydrogens!* This remarkable manifestation results from the convex curvature of the X–X bond path and *seemingly* contradicts the correlation we developed above. In fact, there is no contradiction because the geometrical tilt angle and the convex X–X bond path represent the same phenomenon. Namely, curving the X–X bond path induces tilting of the terminal hydrogens so that the X atoms maintain their preferred, ideal “sp” or “sp²” hybridization.

The question then becomes, Why do the X–X bond paths have convex curvatures? The origin lies in the distortion that the X–X bond undergoes upon 3c–2e bonding, which for

(11) Allred, A. L.; Rochow, E. G. J. *Inorg. Nucl. Chem.* **1958**, *5*, 269–288. Allen, L. C. *J. Am. Chem. Soc.* **1989**, *111*, 9003 and references cited therein.

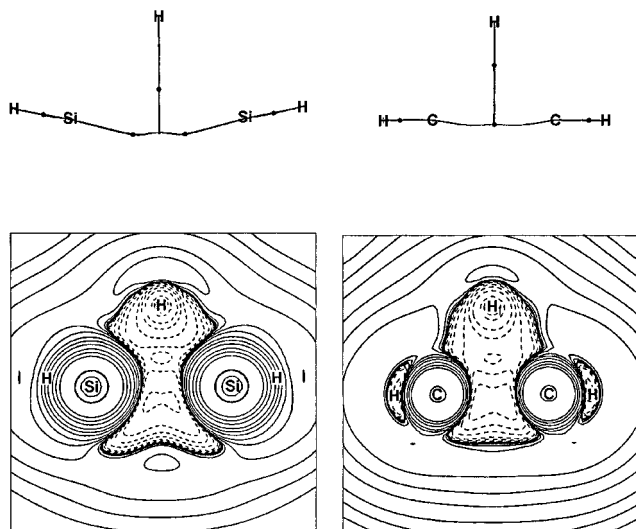


Figure 12. Displays of the molecular graphs (top) and the contour maps of the Laplacian concentration of the charge density (bottom) in the C_s symmetry plane of Si_2H_5^+ (left) and C_2H_5^+ (right) at the MP2/6-311G** level of approximation. In the molecular graphs, projected in the plane, the bond paths are shown by lines and the bond critical points by dots. In the Laplacian contour maps the dashed lines denote negative values of $\nabla^2\rho$ and indicate regions where electronic charge is concentrated.

simplicity can be thought to result from (di)protonation of an $\text{X}=\text{X}$ or $\text{X}\equiv\text{X}$ bond. Intuitively, such an interaction might be expected to give a concave instead of a convex $\text{X}-\text{X}$ bond path, because the bridging proton supposedly pulls electron density. However, it can be illustrated by the properties of both the molecular graphs and the Laplacians $\nabla^2\rho$ (Figure 12) that the bridging hydrogens disperse the electronic charge in the $3c-2e$ region that causes a convex bond path between the heavy elements. This, in fact, is also evident from the relevant molecular orbitals displayed for Si_2H_5^+ in Figure 9.

Except for Al_2H_3^- and the dianions $\text{Be}_2\text{H}_4^{2-}$ and $\text{Mg}_2\text{H}_4^{2-}$, the molecular graphs of all the $3c-2e$ systems are T-shaped with the bridging hydrogens (H_b) having bond paths to the middle of the $\text{X}-\text{X}$ bond paths. The ellipticity (ϵ) of all the H_b-X_2 bond paths at their bond critical points, listed in Table 3, are extremely large, indicating that the electron density (ρ) of these bond paths disperses into the XH_bX plane. This notion is supported by the large ellipticities of the bond critical points and maxima of the $\text{X}-\text{X}$ bond paths of the $3c-2e$ systems of groups A and B. Due to the orthogonality of two $3c-2e$ interactions, negligible ellipticities are obtained for the bond critical points of the $\text{X}-\text{X}$ bond paths of the $\text{X}_2\text{H}_4^{2+0/2-}$ systems of group C. These data are also listed in Table 3.

The Laplacian $\nabla^2\rho$ shows that the electronic charge is indeed dispersed in the three-center XH_bX area. The contour maps of these Laplacian concentrations in the XH_bX plane, shown in Figure 12, illustrate this effect for the representative C_2H_5^+ and Si_2H_5^+ cations. They also highlight the influence of the less electronegative Si on the $\text{X}-\text{X}$ bonding. The same features are evident in the corresponding B_2H_5^- and Al_2H_5^- anions. These anions show an even higher dispersion of electron density around the $\text{X}-\text{X}$ bond. This may not be surprising when it is recognized that both the diborane structures B_2H_6 and Al_2H_6 have, in fact, no $\text{X}-\text{X}$ but only $\text{X}-\text{H}_b$ and $\text{X}-\text{H}_t$ bond paths.

III. Structures and Energies. After having emphasized the special bonding features of the $3c-2e$ systems, it is important to determine whether they indeed fly, *i.e.*, whether they are viable species on their respective potential energy surfaces. While this may speak for itself for the extensively studied

nonclassical ethyl and vinyl cations, the other species are less mundane if not exotic. Still, of the fourteen $3c-2e$ species, eight are minimum energy structures and the other six are transition structures. We discuss for each of the groups A, B, and C some structural aspects and energies, starting with the more conventional species of group A.

Group A: $\text{X}_2\text{H}_5^{+/-}$. All four $3c-2e$ structures ($\text{X} = \text{C}, \text{B}, \text{Si},$ and Al) are minima. The ethyl cation (C_2H_5^+) and the B_2H_5^- anion as well as Si_2H_5^+ and Al_2H_5^- are iso-electronically related. The cations are best viewed as protonated ethylene and silylene (C_{2h}) and the anions as deprotonated diborane(6) and dialane(6), respectively. The corresponding energies are listed in Table 4, entries 7–10. Interestingly, the deprotonation energies are the same for diborane(6) and dialane(6).

These $\text{X}_2\text{H}_5^{+/-}$ structures can also be thought of as complexes between XH_3 and $\text{XH}_2^{+/-}$, analogous to the XH_3 dimerization that leads to the diborane-type structure. Such an interaction, visualized in Figure 13, reinforces the convex nature of the $\text{X}-\text{X}$ bonds but also illustrates that the curvature diminishes (increases) on a stronger (weaker) interaction between the heavy atoms X . This pattern is, in fact, reflected in the diborane-like structures, where the electron density disperses from the center in the order $\text{C}_2\text{H}_6^{2+} < \text{B}_2\text{H}_6 < \text{Al}_2\text{H}_6$.¹²

Group B: $\text{X}_2\text{H}_3^{+/-}$. Only the vinyl cation, protonated acetylene, is a minimum energy structure, while Si_2H_3^+ ,¹³ B_2H_3^- ,¹⁴ and Al_2H_3^- ¹⁵ are $3c-2e$ transition structures (C_{2v}). The nature of these transitions was investigated. Relevant minimum energy structures are displayed in Figure 14; their energies are listed in Table 1. For B_2H_3^- the C_2 -symmetry form, in which the H_t hydrogens are slightly tilted out of the BH_bB plane, is only 0.13 kcal/mol more stable than the C_{2v} -symmetry form. The energetic preference even disappears for this structure, which is only modestly deformed from planarity, when zero-point energy corrections are included in the energy evaluation; the “classical” $\text{H}_2\text{B}=\text{B}$ (C_{2v}) structure is 7.8 kcal/mol less stable than the bridged form. The structural differences are much more pronounced in the dialane anion, which prefers a triply bridged isomer. This D_{3h} -symmetry isomer of Al_2H_3^- is favored by a significant 33.8 kcal/mol over the $3c-2e$ form, which represents a transition structure for H scrambling. Likewise, the Si_2H_3^+ cation prefers the triply bridged conformation (D_{3h}), by as much 43.4 kcal/mol. In contrast, the corresponding D_{3h} isomer of B_2H_3^- is 43.6 kcal/mol less stable than the singly bridged form.

Particularly, the tri-H-bridged Al_2H_3^- can be related to its protonated form, Al_2H_4 . The most stable dialane(4) isomer has a salt-like structure, *i.e.*, $\text{Al}^+\text{AlH}_4^-$ (C_{3v}), in which an Al^+ cation complexes to the face of a tetrahedral AlH_4^- anion.¹⁶ Similarly,

(12) Al_2H_6 and Ga_2H_6 : Lammertsma, K.; Leszczyński, J. *J. Phys. Chem.* **1990**, *94*, 2806. Souter P. F.; Andrews, L.; Downs, A. J.; Greene, T. M.; Ma, B.; Schaefer, H. F. *J. Phys. Chem.* **1994**, *98*, 12824. BAlH_6 , BGaH_6 , and AlGaH_6 : Woerd, M. J. v. d.; Lammertsma, K.; Duke, B. J.; Schaefer, H. F. *J. Chem. Phys.* **1991**, *95*, 1160. $\text{C}_2\text{H}_6^{2+}$: Lammertsma, K.; Olah, G. A.; Barzaghi, M.; Simonetta, M. *J. Am. Chem. Soc.* **1982**, *104*, 6851. B_2H_6 and $\text{C}_2\text{H}_6^{2+}$: Lammertsma, K. Unpublished results. B_2H_6 : Barone, V.; Orlandini, L.; Adamo, C. *J. Phys. Chem.* **1994**, *98*, 13185.

(13) (a) Curtiss, L. A.; Raghavachari, K.; Deutsch, P. W.; Pople, J. A. *J. Chem. Phys.* **1991**, *95*, 2433. (b) Trinquier, G. *Chem. Phys. Lett.* **1992**, *188*, 572. (c) Zyubin, A. S.; Tikilyaine, A. A.; Kaneti, J.; Charkin, O. P. *Zh. Neorg. Khim.* **1986**, *31*, 2495; *Chem. Abstr.* **1986**, *105*, 232689w.

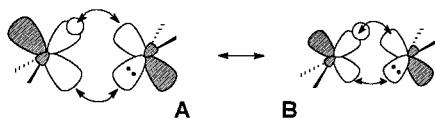
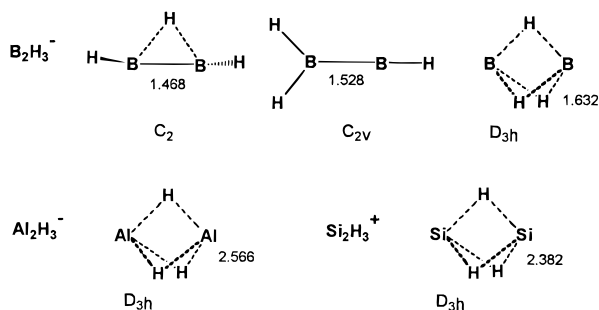
(14) Kirillov, Y. B.; Boldyrev, A. I. *Sovi. J. Coord. Chem.* **1985**, *11*, 429 (Original: *Koord. Khim.* **1985**, *11*, 749). See also: Sana, M.; Leroy, G.; Henriot, C. H. *THEOCHEM* **1989**, *56*, 233. Sana, M.; Leroy, G. *THEOCHEM* **1987**, *36* 307. Bigot, B.; Lequan, R. M.; Devaquet, A. *Nouv. J. Chim.* **1978**, *2*, 449. Kaufmann, E.; Schleyer, P. v. R. *Inorg. Chem.* **1988**, *27*, 3987.

(15) Zyubin, A. S.; Charkin, O. P. *Zh. Strukt. Khim.* **1986**, *27*, 45–58; *Sov. J. Coord. Chem.* **1987**, *13*, 882.

(16) Lammertsma, K.; Güner, O. F.; Drewes, R. M.; Reed, A. E.; Schleyer, P. v. R. *Leszczyński, J. Inorg. Chem.* **1989**, *28*, 313.

Table 4. Protonation and Deprotonation Energies (in kcal/mol) of 3c–2e Systems

entry	process	HF/ 6-31G**	MP2/ 6-31G**	MP2/ 6-311G**	MP2/ 6-311G** + ZPE
1	$C_2H_2 + H^+ \rightarrow C_2H_3^+$	+164.8	+160.6	+157.0	+151.8
	$D_{\infty h} \rightarrow C_{2v}$				
2	$Si_2H_2 + H^+ \rightarrow Si_2H_3^+$	+208.5	+208.6	+211.3	+205.3
	$C_{2v} \rightarrow D_{3h}$				
3	$C_2H_2 \rightarrow C_{2v}$	+165.7	+164.6	+164.8	+161.8
	$B_2H_4 - H^+ \rightarrow B_2H_3^-$				
4	$D_{2d} \rightarrow C_{2v}$	-412.7	-393.4	-376.3	-369.2
	$C_{2v} \rightarrow C_{2v}$				
5	$Al_2H_4 - H^+ \rightarrow Al_2H_3^-$	-393.5	-391.8	-376.8	-369.1
	$C_{3v} \rightarrow D_{3h}$				
6	$C_2H_4 + H^+ \rightarrow C_2H_5^+$	-358.0	-356.1	-357.4	-352.9
	$D_{2h} \rightarrow C_{2v}$				
7	$Si_2H_4 + H^+ \rightarrow Si_2H_5^+$	+177.0	+171.9	+168.9	+162.6
	$C_{2h} \rightarrow C_{2v}$				
8	$B_2H_6 - H^+ \rightarrow B_2H_5^-$	+213.5	+208.6	+209.9	+204.3
	$C_{2h} \rightarrow C_{2v}$				
9	$Al_2H_6 - H^+ \rightarrow Al_2H_5^-$	-375.9	-377.0	-365.8	-356.6
	$C_{2h} \rightarrow C_{2v}$				
10	$C_2H_3^+ + H^+ \rightarrow C_2H_4^{2+}$	-366.1	-365.5	-364.7	-357.6
	$C_{2v} \rightarrow D_{2d}$				
11	$C_{2v} \rightarrow C_{2v}$	+6.9	-24.6	-28.4	-35.8
	$C_{2v} \rightarrow C_{2v}$				
12	$Si_2H_3^+ + H^+ \rightarrow Si_2H_4^{2+}$	-36.7	-40.3	-39.5	-43.1
	$D_{3h} \rightarrow C_{2v}$				
13		+60.2	+49.0	+49.5	+45.7

**Figure 13.** Interaction diagram between XH_3 and $XH_2^{+/-}$: left (A), the lighter elements X with more diffuse orbitals; right (B), the heavier elements with the denser orbitals and tighter interactions.**Figure 14.** Minimum energy isomers of the 3c–2e isomers of group B.

$BAlH_4$, $BGaH_4$, and $AlGaH_4$,¹⁷ but not B_2H_4 (see below),¹⁸ have been characterized as ionic $X^+XH_4^-$ species. The electron density analyses show no X–X bond path for any of these. Likewise, the tri-H-bridged $Al_2H_3^-$ anion (D_{3h}) has no Al–Al bond path. This highlights the weakness in covalent bonding between the two aluminum atoms, which also explains why the 3c–2e $Al_2H_3^-$ structure is the only one in group B to have X–H_b bond paths.

The tendency for H bridging is also prevalent in silynes. Thus, Si_2H_2 has a di-H-bridged structure (C_{2v}) instead of an

acetylenic structure.¹⁹ Protonation occurs at its Si–Si bond to give a tri-H-bridged $Si_2H_3^+$ cation structure (D_{3h}), which contains no Si–Si bond path. The similarity with the dialane $Al_2H_3^-$ anion is evident.

Some of the protonations and deprotonations that yield $X_2H_3^{+/-}$, the energies of which are listed in Table 4, provide further insight. The difference between the Si–Si σ -bond protonation of Si_2H_2 and the π -bond protonation of Si_2H_4 ²⁰ is negligible, as reflected in their respective proton affinities of 205.3 and 204.3 kcal/mol. Both are significantly higher than those of acetylene, 151.8 kcal/mol, and ethylene, 162.6 kcal/mol. The proton affinities of both $B_2H_3^-$ and $Al_2H_3^-$ (entries 5 and 6) are substantial, as might be expected for anions. They are of a magnitude similar to the 357 kcal/mol for both the $B_2H_5^-$ and $Al_2H_5^-$ anions (entries 9 and 10).

Group C: $X_2H_4^{2+/0/2-}$. The three di-H-bridged systems of the first-row elements Be, B, and C are minima, while those of the second row elements Mg, Al, and Si are transition structures; related minimum energy structures are shown in Figure 15, and their energies are given in Table 1. All display intriguing features. For example, the di-H-bridged carbocation $C_2H_4^{2+}$ (C_{2v}) can be viewed (a) as a diprotonated acetylene, with the two protons immersing into the orthogonal π orbitals of the triple bond, or (b) as a protonated vinyl cation, with the proton immersing into the π orbital that is orthogonal to the vinyl 3c–2e interaction. Confirming earlier studies on the $C_2H_4^{2+}$ dications,²¹ we find that this di-3c–2e system (C_{2v}) is less stable than the perpendicular $H_2C-CH_2^{2+}$ (D_{2d}) isomer (Figure 15), but the energy difference of 7.3 kcal/mol between the two minimum energy structures is remarkably small. Of the two neutral B_2H_4 species, the di-H-bridged structure is, in fact, more stable than the perpendicular covalent H_2B-BH_2 (D_{2d}) isomer even though this energy difference is only 0.65 kcal/mol

(17) Leszczyński, J.; Lammertsma, K. *J. Phys. Chem.* **1991**, *95*, 3941. Lammertsma, K.; Leszczyński, J. *J. Phys. Chem.* **1990**, *94*, 5543.

(18) Stanto, J. F.; Gauss, J.; Bartlett, R.; Helgaker, T.; Taylor, P. R. *J. Chem. Phys.* **1992**, *97*, 1211. Mohr, R. R.; Lipscomb, W. N. *Inorg. Chem.* **1986**, *25*, 1053.

(19) Grev, R. S.; Schaefer, H. F. *J. Chem. Phys.* **1992**, *97*, 7990. Bogey, M.; Bolvin, H.; Demuyneck, C.; Destombes, J. L. *Phys. Rev. Lett.* **1991**, *66*, 413. Colegrove, B. T.; Schaefer, H. F. *J. Phys. Chem.* **1990**, *94*, 5593. Binkley, J. S. *J. Am. Chem. Soc.* **1984**, *106*, 603. For Al_2H_2 , see: Palágyi, Z.; Grev, R. S.; Schaefer, H. F. *J. Am. Chem. Soc.* **1993**, *115*, 1936. Ga_2H_2 : Palágyi, Z.; Schaefer, H. F. *J. Am. Chem. Soc.* **1993**, *115*, 1936. Ge_2H_2 : Palágyi, Z.; Schaefer, H. F.; Kapuy, E. *J. Am. Chem. Soc.* **1993**, *115*, 6901.

(20) Si_2H_4 : Luke, B. T.; Pople, J. A.; Krogh-Jespersen, M.-B.; Apeloig, Y.; Karni, M.; Chandrasekhar, J.; Schleyer, P. v. R. *J. Am. Chem. Soc.* **1986**, *108*, 270. Olbrich, G. *Chem. Phys. Lett.* **1986**, *130*, 115. Sannigrahi, A. B.; Nandi, P. K. *Chem. Phys. Lett.* **1992**, *188*, 575.

(21) $C_2H_4^{2+}$: Lammertsma, K.; Barzaghi, M.; Olah, G. A.; Pople, J. A.; Kos, A. J.; Schleyer, P. v. R. *J. Am. Chem. Soc.* **1983**, *105*, 5252. Nobes, R. H.; Wong, M. W.; Radom, L. *Chem. Phys. Lett.* **1987**, *136*, 299. Wong, M. W.; Yates, B. F.; Nobes, R. H.; Radom, L. *J. Am. Chem. Soc.* **1987**, *109*, 3181.

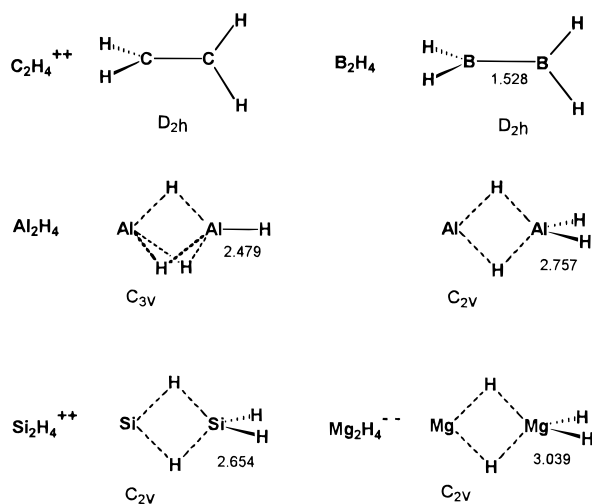


Figure 15. Minimum energy isomers of the 3c-2e isomers of group C.

(without the ZPE correction), a result that is analogous to a recent study on these two species.¹⁸ The near isoenergetics of these two isomers may explain why no B_2H_4 species has yet been characterized experimentally.

The di-H-bridged structures of the $Si_2H_4^{2+}$ dication and the neutral Al_2H_4 represent both transitions for a degenerate H rearrangement. The associated minimum energy structure of the $Si_2H_4^{2+}$ dication (C_{2v}) can be viewed as a π -diprotonated silylidene, $H_2Si=Si$, while that of Al_2H_4 represents a salt-like structure with an Al^+ cation complexed to the edge of an AlH_4^- anion (C_{2v}).¹⁶ The respective barriers for H transfer are 33.7 kcal/mol for $Si_2H_4^{2+}$ and 22.8 kcal/mol for Al_2H_4 . These barriers are 10 kcal/mol less for both the related H-scrambling barriers ($D_{3h} \rightarrow C_{2v}$) of 33.8 kcal/mol for $Al_2H_3^-$ and 43.4 kcal/mol for $Si_2H_3^+$. Neutral Al_2H_4 has a slightly more stable triply bridged form (C_{3v}). This isomer can be viewed as having an Al^+ cation complexed to the face of the tetrahedral AlH_4^- anion.¹⁶

The dianionic di-H-bridged structures of the second group of the periodic table behave as those of groups 3 and 4. Thus,

$Be_2H_4^{2-}$ is a minimum energy structure analogous to those of the first-row elements, while the $Mg_2H_4^{2-}$ form represents a transition structure in analogy to the di-H-bridged structures containing the second-row elements Al and Si. Also $Mg_2H_4^{2-}$ has a minimum energy structure of C_{2v} symmetry, which, like those of Al_2H_4 and $Si_2H_4^{2+}$, does not contain a X-X bond path.

Conclusions

This study is concerned with species that display three-center, two-electron bonding. Common bonding patterns are found for a broad group of such systems that include mono- and dications, mono- and dianions, and neutral molecules that contain eight different elements of the first and second rows of the periodic table. The parent systems studied are $X_2H_3^{+/-}$ (C, B, Si, Al), $X_2H_5^{+/-}$ (C, B, Si, Al), and $X_2H_4^{2+/-}$ (C, B, Be, Si, Al, Mg). All but two of these have their hydrogens on one side of a plane that contains both heavy elements. Accordingly, these elements have inverted geometries. The geometrical tilt angles of the terminal hydrogens can be quite significant. They become larger when the 3c-2e systems contain the more electropositive elements. *These geometrical tilt angles correlate linearly with Allred and Rochow's elemental electronegativities.* The bond lengths between the heavy elements also correlate with the tilt angles. The origin of these angles is traced to a mixing of the π (X-X) and σ ($XH_{(2)}$) orbitals. These two orbitals combined show a more diffuse nature in the H-bridging area. This is substantiated by the one-electron density analysis, which shows that the electronic structures of the 3c-2e species have no tilt angles between the X-H_i and X-X bonds. Instead, molecular graphs show that the X-X bonds have convex curvatures. They further show that the bridging hydrogens have bond paths directly to the centers of these convex X-X bonds.

Acknowledgment. This work was supported by the U.S. Air Force Office of Scientific Research under F49620-94-1-0451. T.O. acknowledges the Yamada Science Foundation for financial support for a study visit. The Alabama Supercomputer Center is acknowledged for generous allotment of computer time. Mr. M. v. d. Woerd is thanked for his early contributions.

JA960004X